



STRUCTURAL IMPACT SIMULATION USING PROGRAM KRASH

SAE 900466

INTERNATIONAL CONFERENCE ON EMERGING TECHNOLOGIES IN VEHICLE CAE & STRUCTURAL MECHANICS - DETROIT

J.C.Liaw
Cranfield Institute of Technology

A.C.Walton
Cranfield Impact Centre Ltd

J.C.Brown
Cranfield Impact Centre Research
Cranfield Institute of Technology

College of Aeronautics
Cranfield Institute of Technology
Cranfield, Bedford MK43 0AL. England



Cranfield

College of Aeronautics Report No.9010
1992



STRUCTURAL IMPACT SIMULATION USING PROGRAM KRASH

SAE 900466

INTERNATIONAL CONFERENCE ON EMERGING TECHNOLOGIES IN
VEHICLE CAE & STRUCTURAL MECHANICS - DETROIT

J.C.Liaw
Cranfield Institute of Technology

A.C.Walton
Cranfield Impact Centre Ltd

J.C.Brown
Cranfield Impact Centre Research
Cranfield Institute of Technology

College of Aeronautics
Cranfield Institute of Technology
Cranfield, Bedford MK43 0AL. England

ISBN 1 871564441

£8.00

"The views expressed herein are those of the authors alone and do not necessarily represent those of the Institute"

Structural Impact Simulation Using Program KRASH

J. C. Liaw
Cranfield Institute of Technology

A. C. Walton
Cranfield Impact Centre, Ltd.

J. C. Brown
Cranfield Impact Centre Research
Cranfield Institute of Technology

ABSTRACT

Use is made of the KRASH program to simulate a simplified car-into-barrier impact. A step-by-step modelling technique is illustrated whose application at an early stage in the design process, allows an understanding of the contribution of individual components to the overall crash-performance of a vehicle.

INTRODUCTION

The use of computer-based, analytical methods to predict the crash-characteristics of a proposed vehicle has become a fundamental part of the design process. An increasing number of programs are available for this purpose which vary in complexity from simple one-dimensional, lumped-mass codes through to three-dimensional Finite Element (FE) programs which allow detailed models to be run.

In broad terms, these programs allow two different types of approach to be made to structural impact modelling. The first involves the use of a 'complex' FE program to model the structure in detail, using only geometric and material-properties data. (The input for this model may come directly from the linear-elastic analysis of the vehicle conducted during the design process.) In its most detailed form, this type of model requires super-computer power to carry out the large amount of equation-solving which is required.

The second approach is commonly termed 'hybrid' because it involves combining the results of structural component tests into a simplified FE model. The hybrid approach requires the user to identify components in the structure which will play a significant role in the collapse process. Having identified these components (and their anticipated direction of collapse - ie. crushing, bending, torsion or shear) tests are carried out to determine

their force versus deflection characteristics.

In general, the hybrid method requires considerably less computing resources than the full FE approach. This is because the non-linear characteristics of components which are obtained by test are stored in the program and are recalled when an element is stressed beyond its elastic limit. Consequently, the method avoids the need to carry out large amounts of equation-solving to predict this non-linear behaviour. More recently, the distinction between 'full' FE and hybrid approaches has become obscure as a number of full programs now include a hybrid facility.

This paper uses the KRASH hybrid structural dynamics program to simulate a simplified car structure in a frontal barrier impact at 35mph. The objectives of this paper are as follows:

(a) to outline an approach to the simulation of vehicle structural impact-dynamics through the use of a simplified frontal impact model
(b) to identify, through the use of the model, structural features which determine the crash-behaviour of a car in a frontal barrier impact

(c) to identify current limitations of the approach and to outline future improvements.

A step-by-step method is used in this paper to model the vehicle impact. The simulation begins with a simplified single-mass model and is successively repeated with further additions of structural detail at each stage. This technique is in direct contrast to the creation and running of a single highly-detailed model. The reason for using this incremental approach is that the effect of each addition to the model can be assessed. This advantage can be illustrated by reference to the acceleration time-history at the driver's seat base which is one of the primary pieces of output information required from an impact model. This signal will control the degree of injury experienced by the driver (excluding intrusion effects) and, where necessary, it is this signal which

will have to be modified (via structural changes) to reduce the injury-level. However, the transient, almost random-like, nature of the signal makes it difficult to interpret which structural member(s) causes a particular deceleration peak. A step-by-step approach allows the effects of individual members on the overall crash-signal to be assessed. Furthermore, this technique also has the advantage of allowing the user to identify elements in the model which cause solution-instability and to verify that individual elements are not developing faults during the course of the simulation.

Before proceeding with a description of the model used in the study, the KRASH program is briefly described below.

DESCRIPTION OF THE KRASH PROGRAM

KRASH is a three-dimensional 'hybrid' structural-dynamics code which has been written for the simulation of aircraft and helicopter impacts. The program has been extensively used and validated in the analysis of airframe crashworthiness and continues to be developed under the funding of the US Federal Aviation Administration (1-5). At Cranfield Impact Centre, KRASH has been applied to a variety of different impact problems under commercial constraints including car-into-barrier, car-into-truck, car-into-highway guard-rails and aircraft crashes.

The program requires the user to idealise the structure of interest into a series of mass points which are linked together by deformable beams. The weight of the structure is distributed amongst the lumped-mass points whilst the beams are given the collapse characteristics of the intervening sections of structure. In this way, a model can be built up which represents the weight, inertia, stiffness and non-linear collapse characteristics of the vehicle structure.

The hybrid nature of the program allows direct input of information defining the collapse-behaviour of chosen components. KRASH works by repeatedly setting-up and solving the equations of motion for each of the lumped mass points using an explicit equation-solving routine. The course of the impact is simulated as the procedure steps through the whole duration of the impact. Further details of the theory of the program can be found in references (6)* and (7).

DESCRIPTION AND APPLICATION OF MODEL

The model reported in this paper represents a car of total mass 1000kg (2204.62 lbf weight) striking a rigid, immovable barrier at 15.65 metre/sec (m/s), (35mph). The engine of the car accounted for 200kg (440.93 lbf) of the total mass. The car had a total frontal struc-

ture length of 1.0 metre (m), (39.37 in) with its centre of gravity, 'cg', being 2.0m (78.74 in) from the front of the vehicle. The cg of the model was assumed to correspond to the longitudinal position of the accelerometer at the base of B-Post and the time-histories predicted at this point were used as a basis for comparison throughout this study.

In order to test the ability of the program to simulate over large values of structural deformation, it was arbitrarily chosen that the structure would collapse through a distance of 0.75m (29.53 in). Additionally, it was decided that the structure would collapse at a constant load. By equating the kinetic energy of the vehicle to the work done during the impact, this gave a constant total collapse force of 163207N (36691 lbf), (or 81603N (18345 lbf) per side-member). Under these conditions, the cg of the car would receive a constant deceleration of 16.64g for a duration of 96 milliseconds (1.0ms = 0.001 secs) before rebounding from the barrier. In normal design practice, the required deceleration signal would determine the necessary collapse distance (and force) and would itself be dictated by occupant-injury criteria.

Throughout each of the parametric runs conducted in this study, the collapse force of each forward longitudinal was kept at the constant value of 81603N. The total mass of the car was also kept at a constant 1000kg although the distribution of the mass was changed as a consequence of defining the engine (and other parts of the structure) as separate items.

The parameters investigated are outlined below:

- (1) Single mass model - Baseline Model
- (2) Model with structural mass at car/barrier interface
- (3) Model with rigidly-mounted engine - engine of zero volume
- (4) Model with rigidly-mounted engine - engine of finite volume
- (5) Model with low breakage-strength engine mounts
- (6) Model with high breakage-strength engine mounts
- (7) Model with high breakage-strength engine mounts plus front wheels
- (8) Model with high breakage-strength engine mounts plus front wheels at low impact speed.

(1) BASELINE MODEL - The baseline model is illustrated in Fig 1(a) and constituted the simplest model of the car. It was comprised of a single lumped-mass of 1000kg (representing the total mass of the vehicle²) with two contact springs modelling the constant collapse-force of the two longitudinals.

The use of contact spring elements in KRASH is significant in that mass cannot be located at the barrier-interface end of a spring. Hence, the inertia of the longitudinals was not included in this model.

The acceleration (filtered), velocity and displacement time-histories of the cg of the model are shown in Fig 2. From the 'square-wave'

* Numbers in parentheses designate references at end of paper.

nature of the acceleration curve, it was clear that the acceleration experienced at the cg was directly controlled by the collapse characteristics of the left and right-hand longitudinals. The magnitude and duration of the deceleration signal at the cg corresponded with the value of 16.6g for 96ms, as derived by the initial hand-calculation.

The value of damping in the left and right-hand contact springs was set to zero (damping being input in terms of the ratio actual damping/critical damping). Previous studies have shown that the value of damping chosen for an element has a fundamental effect on the force developed by that element - KRASH uses linear-viscous damping.

In order to examine the effect of increased element damping on the cg time-histories, the baseline model was repeated with the spring damping-ratio set to 1% and 10% in succession. The resulting cg time-histories are shown in Figs 3 and 4 respectively. Peak decelerations were raised from a constant 16.6g of the baseline to 32g (and 130g) respectively, whilst velocity rebound times were reduced from a baseline value of 96ms to 65ms (and 22ms) respectively. The force time-history of the left-hand spring is shown in Fig 5 for the 10% damping case - it is identical to the unfiltered cg acceleration time-history which is superimposed on top of it.

(2) MODEL WITH STRUCTURAL MASS AT CAR/BARRIER INTERFACE - This model copied the baseline model with the exception that a beam element was used in place of a spring to represent each longitudinal, Fig 1(b). This substitution allowed mass to be placed near to the car/barrier interface. A mass of 20kg (44.09 lbf) was located at the impact end of each longitudinal to represent the inertia of the car's forward structure. The intention of this was to examine the effect that the presence of mass at this forward point in the model would have on the cg behaviour. By having to use the beam element in order to include the presence of mass, the replacement of the spring element resulted in a second parametric change.

As KRASH requires the use of a spring to generate contact between the vehicle and barrier, a spring was added to the front of each longitudinal. Each spring was given a highly stiff, linear-elastic characteristic so as not to add to the energy-dissipation capacity of the two longitudinals. (In this case, the springs acted as part of the barrier rather than part of the car). The beam damping ratio was set to zero to maintain consistency with the baseline model.

The acceleration (filtered), velocity and displacement time-histories of the cg are shown in Fig 6. Comparison with the baseline values (Fig 2) showed an overall similarity in the square-wave shape of the acceleration pulse. However from 15ms onwards, the acceleration signal of this model began to oscillate

about an increasing average value, reaching a maximum of some 22g by 80ms. As before, the unfiltered acceleration time-history of the cg corresponded directly with the force time-history in the longitudinals. The oscillatory part of the cg acceleration signal was generated by the 20kg mass and stiff contact spring in combination, repeatedly loading and unloading at the barrier/car interface. Examination of the force/deflection behaviour of each longitudinal (Fig 7) indicated that under repeated 'loading-partial unloading-reloading' conditions, the beam element did not return to its programmed constant collapse load, but returned to a marginally higher load at each reloading stage. This behaviour is currently being studied further: - it should be noted that this is only significant where repeated loading/unloading of a beam occurs.

(3) MODEL WITH RIGIDLY-MOUNTED ENGINE - ENGINE OF ZERO VOLUME - As a development of the previous model, the mass of the engine (200kg, 440.92 lbf including gear box) was subtracted from the total vehicle cg mass. The engine mass was located half-way along the frontal structure of the car (0.5m, 19.69 ins), on the centre line of the vehicle, Fig 1(c). The single beam element of the previous model representing the longitudinal was consequently divided into two elements, (these being referred to as the front and rear longitudinals).

In order to obtain a measure of the effect of the mass of the engine on the cg behaviour, the engine was defined as having 'zero volume' - that is, the shape of the engine was not defined and hence could not generate contact forces. The engine was attached to the mid-points of the longitudinals by perfectly-rigid links representing unbreakable connections between the mass of the engine and the structure.

The acceleration (filtered), velocity and displacement time-histories of the cg can be seen in Fig 8. The acceleration pulse maintained a basic square-wave shape (in the region of 18-20g) up to 60ms; whereafter the square-wave broke down. The time to rebound from the barrier increased by approximately 15ms over the previous 'no-engine' model - an apparent reduction in severity. (However, it should be remembered that the previous model developed a beam-error which resulted in higher-than-intended levels of deceleration being generated.) The unfiltered cg acceleration signal (Fig 9) was identical in shape to the force time-history of the rear longitudinal (Fig 10) which connected the engine to the cg of the car.

The unfiltered acceleration signal could itself be divided into a number of different regions (Fig 9). The first consisted of an oscillatory square-wave lasting to 40ms. This was caused by the rapid loading and unloading of the high frequency spring/mass system at the front of the longitudinal. This induced continual collapse of the forward longitudinal to the extent that it developed high stiffness due to total compression at 40ms. The force-time history of this member (Fig 11) illustrates

the 'bottoming out' at 40ms. The high force generated by this action initiated collapse in the rear longitudinal, resulting in collapse of this latter member from 40ms on to 60ms - this can be seen as the continuous value of 22g seen at the cg from 40 to 60ms in Fig 9. The difference in timing between the axial collapse of the front and rear longitudinals can be seen in Fig 12.

In the range 60 to 70ms, the unfiltered acceleration signal entered a high-frequency oscillation phase (Fig 9). This oscillation indicated near-zero acceleration on the cg and represented free elastic vibration over this time, a view reinforced by the zero-reduction in velocity of the cg from 60 to 70ms (Fig 8). This short zero-state can be explained by examining the displacement-history of the engine (Fig 13, dashed-line). From the start of the impact, the engine's motion was forwards - the engine rebounded from the barrier when the forward longitudinal bottomed-out at 40ms. The rebound of the engine was resisted by the rear longitudinal (under compression from the forward motion of the car's cg) until the engine's velocity was reversed towards the barrier at 55ms. During this second forward motion of the engine, the rear longitudinal unloaded, resulting in the short zero-acceleration state at the cg between 60 and 70ms.

The pulse experienced by the cg between 70 and 80ms and again between 85 and 95ms was due to the repeated forward-rearwards motion of the engine.

(4) MODEL WITH RIGIDLY-MOUNTED ENGINE - ENGINE OF FINITE VOLUME - This simulation followed the previous model with the exception that, in this case, the volume of the engine was defined. The intention of this change was to examine whether the incompressible bulk of the engine would act to restrict the collapse of the longitudinals. In the preliminary design of a car, the frontal longitudinals are often considered to be the primary means of dissipating crash-energy. The presence of the engine block can limit the collapse of the longitudinals, resulting in large deceleration levels being subjected on the passenger cell.

In this simulation, the engine was modelled as an incompressible block of length 0.75m (29.53 in) whose cg was located at the mid-length of the car's frontal structure. In order for the front of the engine to react against the barrier, a stiff, linear-elastic spring was used to model the front half of the engine-block. To simulate interaction between a rearwards-displaced engine and the firewall, a linear-elastic beam was used to model the back of the engine. Both the spring and beam elements contained 'dead-spaces' to represent clearances in front and behind the engine prior to contact. The model is illustrated in Fig 1(d).

The acceleration (filtered), velocity and displacement time-histories of the model's cg are shown in Fig 14. Examination of the unfiltered cg time-history shows close matching with

the force time-history of the rear longitudinal when compared on the same time-basis (Fig 15). However, from 20ms onwards, a divergence between these two signals was apparent as the level of deceleration increased. Comparison of the cg unfiltered acceleration signal with the force time-history of the beam modelling engine-to-firewall contact demonstrated that this inter-action was responsible for the increase in cg deceleration (Fig 16).

The inclusion of the engine's incompressible volume into the model increased the severity of the impact. The magnitude of this increase is a function of the size of the engine and the stiffness and strength of the bulkhead - (a relatively low elastic stiffness of 175000N/m (1000 lb/in) was chosen for this model).

The short, near-zero acceleration phases experienced by the cg at around 40ms and 65ms were due, as in the previous model, to the forwards and backwards movement of the engine under forces exerted in turn by the barrier and firewall.

The cg of the vehicle rebounded from the barrier at 74ms in comparison with a less-injurious time of 96ms for the previous 'no-engine-volume' model. The detrimental effect of the engine volume was also measured in terms of peak deceleration which reached 26g in this case compared with 22g in the previous model.

(5) MODEL WITH LOW BREAKAGE-STRENGTH ENGINE MOUNTS - This model followed the previous case with the exception that the engine was not rigidly-mounted but was attached to the structure via two mounts (left and right-hand), each of breaking strength 9810N (1.0 tonne, 2204.6 lbf).

The previous models had demonstrated the contribution of the engine to the overall deceleration of the vehicle, (where the engine was rigidly-attached to the structure). As an engine-mount can withstand only a limited force before breaking, the significance of engine-mount breaking load was examined.

In terms of modification to the model, a beam element was used to represent each engine mount in place of the rigid-connection used previously. This required the inclusion of an additional mass-point at the mid-length of the left and right longitudinals, Fig 1(e). (A mass of 20kg (44.09 lbf) was used for each of the two points and was subtracted from the total cg mass to maintain a constant vehicle weight.)

The acceleration (filtered), velocity and displacement time-histories are shown in Fig 17. The engine-mounts broke almost instantaneously (5ms after impact) due to the engine moving forward under its own inertia relative to the vehicle structure.

The saw-tooth oscillation of the filtered acceleration signal up to 56ms was due to the repeated unloading-reloading of the front contact spring (Fig 18). It can be seen from this that the front of the vehicle finally rebounded from the barrier at 58ms, some 2ms after the

cg of the vehicle began moving away from the barrier. The oscillation seen in the filtered acceleration signal after this time was due to free elastic vibration in the front and rear longitudinals as the structure moved away from the barrier.

Examination of the acceleration and velocity time-histories showed that this impact was more severe than the previous case, with a peak deceleration of 40g and a rebound time of 56ms (compared with 26g and 74ms seen previously).

As in the previous model (where engine-volume was included), the deceleration recorded at the cg resulted from a combination of the forces in the rear longitudinal and those from the engine-to-firewall interaction (Fig 19). The early release of the engine from the structure resulted in the forward longitudinal dissipating less of the engine's kinetic energy than previously. As before, the front of the engine struck the barrier, causing the engine to rebound into the firewall. In this model, however, the higher rebound kinetic energy of the engine caused greater compression of the firewall, resulting in a higher level of deceleration being generated from this contact.

(6) MODEL WITH HIGH BREAKAGE-STRENGTH ENGINE MOUNTS - In order to pursue the effect of increasing the engine mount breakage-strength, this model repeated the previous simulation with the strength increased to 98100N (10.0 tonne, 22046.0 lbf), Fig 1(f).

This resulted in the mounts separating at a time of 14.5ms - sufficient for the frontal longitudinals to be crushed to a greater degree than in the previous case, dissipating more of the engine's kinetic energy at an earlier stage in the impact. As a consequence of this, the forces between the engine and the firewall were reduced when contact was made at a later stage in the impact.

The acceleration (filtered), velocity and displacement time-histories are shown in Fig 20. In overall terms, the high-strength mounts resulted in a slightly less severe impact (38.7g peak at the cg) than was seen in the previous model (40.3g).

(7) MODEL WITH HIGH BREAKAGE-STRENGTH ENGINE MOUNTS PLUS FRONT WHEELS - A previous study (8) had indicated that the compression of the front wheel within the wheel-arch of a vehicle may form a significant load-path in a frontal impact. In order to investigate this effect, the previous model was modified to include simplified front wheels. It was assumed that the centre of each wheel was rigidly connected to the engine block - this represented a front-wheel-drive car with an infinitely-strong, transmission link between the wheels and the gearbox.

The front wheels were further assumed to be of 0.5m (19.69 in) diameter and, arbitrarily, of linear stiffness 1750000N/m (10000 lb/in) - with hindsight, this latter value was probably an overestimate of the approximate crush-characteristics of a wheel and tyre. The front half of the wheel was represented by a contact spring

whilst the rear half was represented by a beam element which would interact with the rigid face at the rear of the wheel-arch, Fig 1(g). Dead-spaces were included in both the spring and beam elements to allow for the clearances in front and behind the wheels.

The acceleration time-history consisted of an initial, square-wave retardation of 20g for a period of 25ms. Thereafter, the signal consisted of two major peaks of 120g and 85g which were generated by the compression of the elements which represented the rear-half of the wheels (Fig 22). The two peaks resulted from the engine rebounding twice between the barrier and the firewall.

It was found that the spring modelling the front of the wheel did not contact the barrier during the impact. This came about as a result of the wheel being rigidly-attached to the engine. As the engine moved forwards under its own inertia towards the barrier (carrying the wheels with it), the incompressible length of the engine-block prevented the front of each wheel from contacting the barrier. The rear half of the wheels were compressed however, resulting in the large deceleration peaks seen at the cg.

(8) MODEL WITH HIGH BREAKAGE-STRENGTH ENGINE MOUNTS PLUS FRONT WHEELS (LOW SPEED) - The final simulation in this series was conducted to answer the question 'what acceleration does a vehicle generate at low speed if it has been designed for a higher-speed impact?' The previous model was re-run at an impact speed of 4.47m/s (10mph) without further structural changes.

The results of this are shown in the acceleration (filtered), velocity and displacement time-histories (Fig 23). A retardation of 20g was not exceeded, corresponding with the initial magnitude of deceleration experienced in the previous higher-speed impact. This value of deceleration was controlled by the collapse forces of the forward and rear longitudinals. The energy of the impact was insufficient to cause either the engine to impact the firewall, or the wheels to impact the rear of the wheel arches.

The conclusion to be drawn from this is that the maximum load of an element in the structure will determine the peak deceleration, irrespective of impact speed (neglecting the inclusion of strain-rate effects). Impact speed, on the other hand, determines the extent of the collapse of each element.

CONCLUSIONS

(1) In order to be most cost-effective, crashworthiness analysis techniques have to be applied from the earliest possible stage in the design process.

(2) The use of a simplified model at an early stage helps to reduce the complexities of non-linear structural-dynamic behaviour to a level which is readily understood. To this end, data defining principal structural members, major mass items and so on, can be rapidly

assembled using knowledge of previous vehicles. Parameters which cannot be given a known value at an early stage can be assigned an upper and lower value, allowing a boundary of performance to be predicted.

(3) The progressive, step-by-step development of a simple model allows the contribution of each addition or modification to be assessed. Using this technique, changes to the model which adversely affect occupant-safety can be identified. (Cranfield are developing post-processing programs which will assist the user in determining cause-and-effect in this area.) Additionally, elements which cause problems in terms of solution-stability can also be identified.

(4) Misbehaviour of individual elements (due to program errors or poor input-data) can fundamentally affect models and yet can remain undetected if the overall results appear 'reasonable', whilst the checking of element behaviour by inspection is possible with smaller models, a more satisfactory solution for large models is an automatic, post-processing checking technique - this is currently being investigated at Cranfield.

In addition to element-misbehaviour, the value of damping chosen by the user can considerably modify element behaviour, particularly where damping in the model is of the viscous type (ie. proportional to velocity). Damping is used as a means of dissipating energy from the model which, in reality, is lost due to factors such as friction within the structure. Typically, energy lost due to damping is assumed to account for a small amount (5%) of the total vehicle energy. Little data exists to guide the user on appropriate damping values and it is relatively easy to choose an arbitrary value without realising the consequences of this in terms of element forces.

ACKNOWLEDGEMENTS

The authors would like to thank Gil Wittlin and Max Gamon of Lockheed and the FAA for their support in the use of KRASH.

REFERENCES

- (1) WITTLIN G., GAMON M.A. 'A Method of Analysis for General Aviation Airplane Structural Crashworthiness'
FAA Report No: FAA-RD-76-123. September 1976
- (2) WITTLIN G., GAMON M.A., LaBARGE W.L. 'Full Scale Crash Test Experimental Verification of a Method of Analysis for General Aviation Airplane Structural Crashworthiness'
FAA Report No: FAA-RD-77-188. February 1978
- (3) WITTLIN G., LACKEY D. 'Analytical Modelling of Transport Aircraft Crash Scenarios to Obtain Floor Pulses'
FAA Report No: DOT/FAA/CT-83-23. April 1983

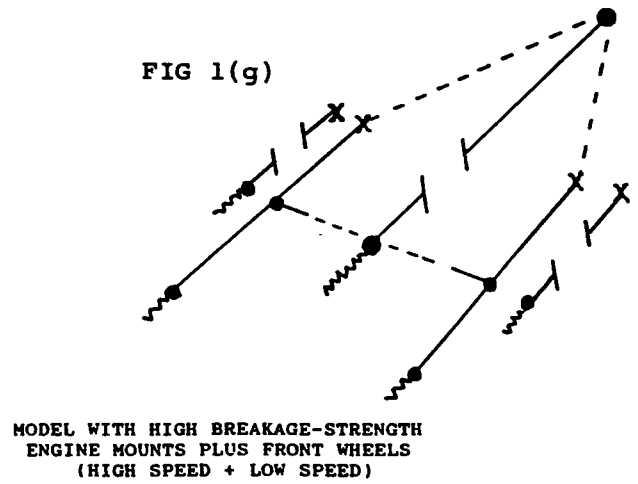
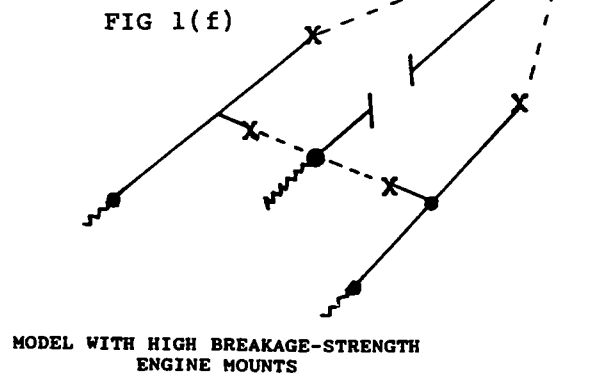
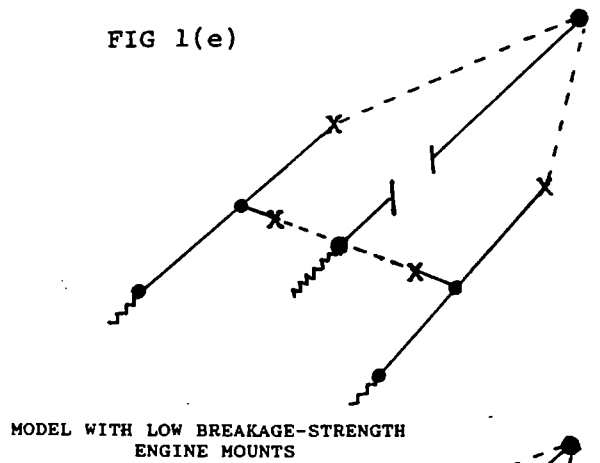
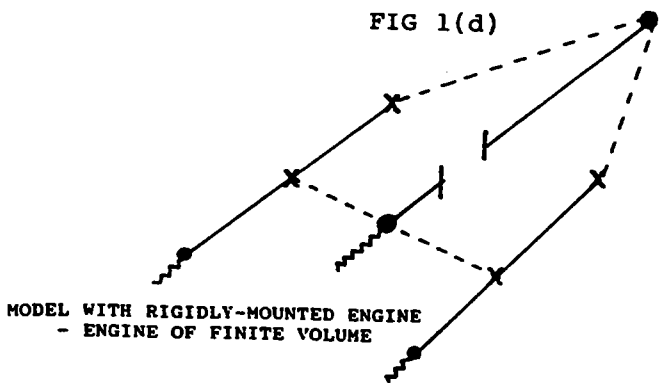
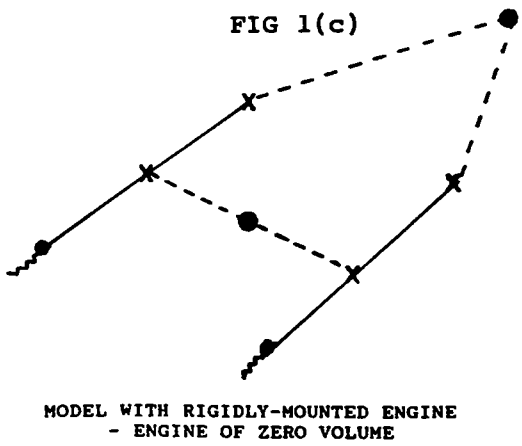
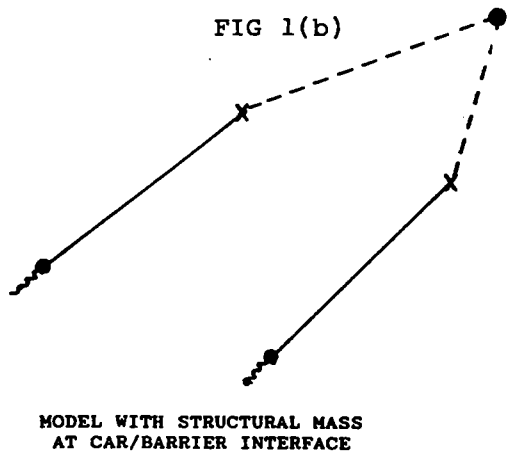
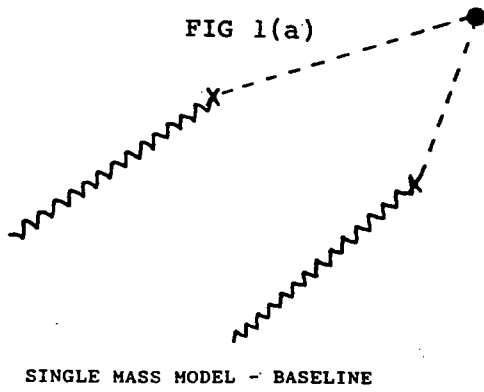
(4) WITTLIN G. 'KRASH Analysis Correlation - Transport Airplane Controlled Impact Demonstration Test'
FAA Report No: DOT/FAA/CT-86/13. December 1986

(5) WITTLIN G., LaBARGE W.L. 'KRASH Parametric Sensitivity Study - Transport Category Airplanes'
FAA Report No: DOT/FAA/CT-87/13. October 1987

(6) GAMON M.A. 'Program "KRASH" Theory'
FAA Report No: FAA-RD-77-189,1. February 1978

(7) GAMON M., WITTLIN G., LaBARGE W.L. 'KRASH 85 User's Guide - Input/Output Format'
FAA Report No: DOT/FAA/CT-85/10.
Revised Edition - March 1986

(8) LIAW J.C. 'The Effect of Structural Parameters on Vehicle Front Impact Behaviour'
MSc Thesis, Cranfield Institute of Technology, UK. September 1988.



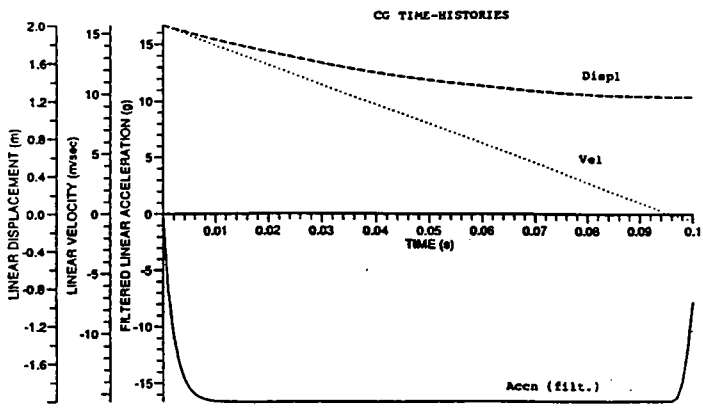


FIG 2

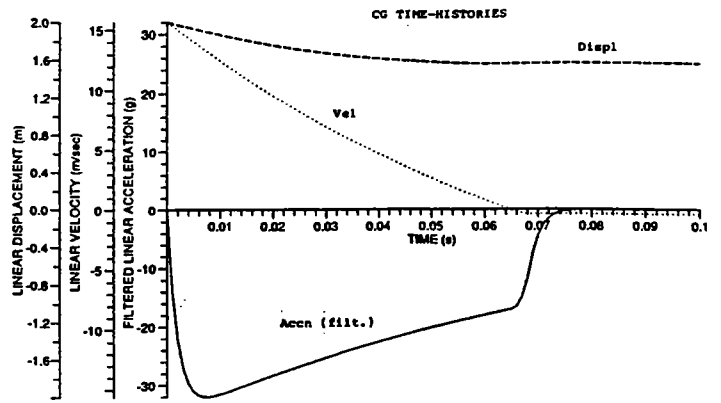


FIG 3

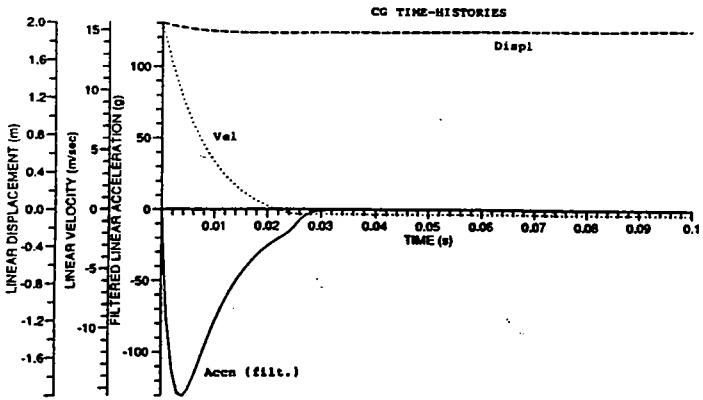


FIG 4

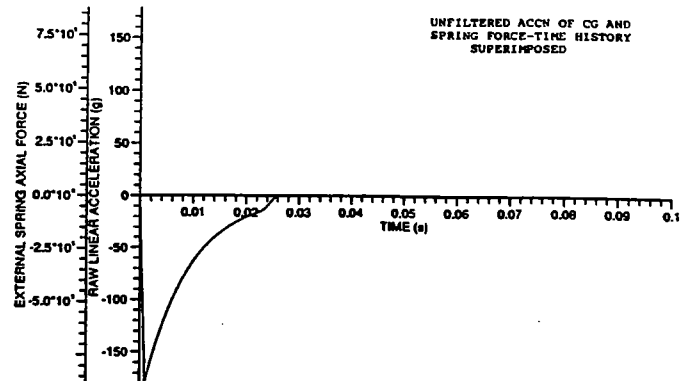


FIG 5

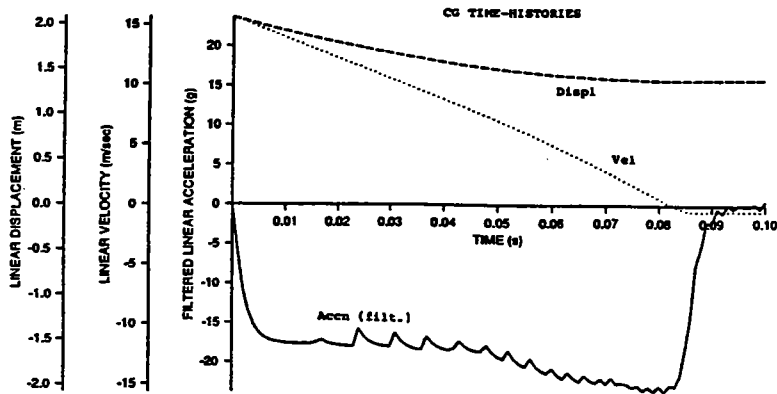


FIG 6

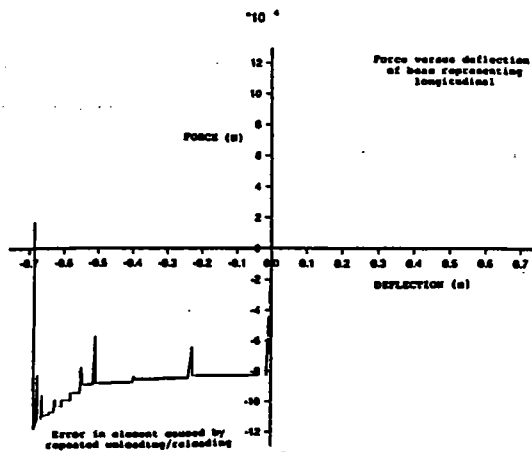


FIG 7

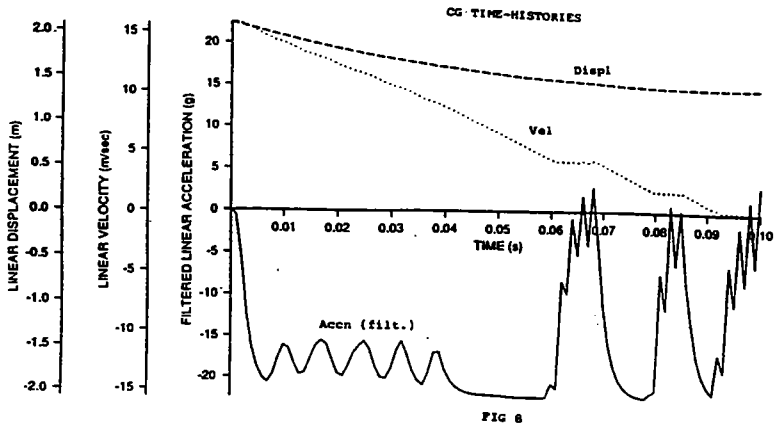


FIG 8

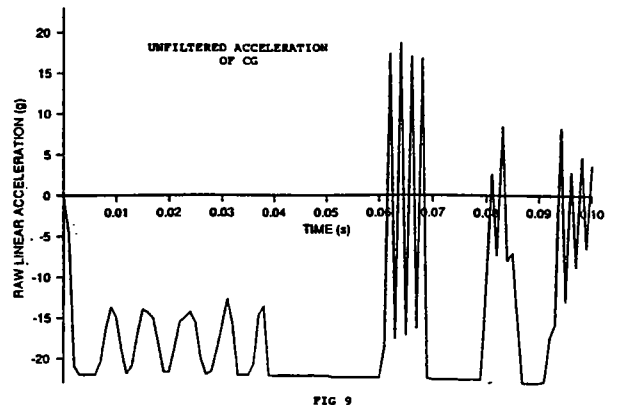


FIG 9

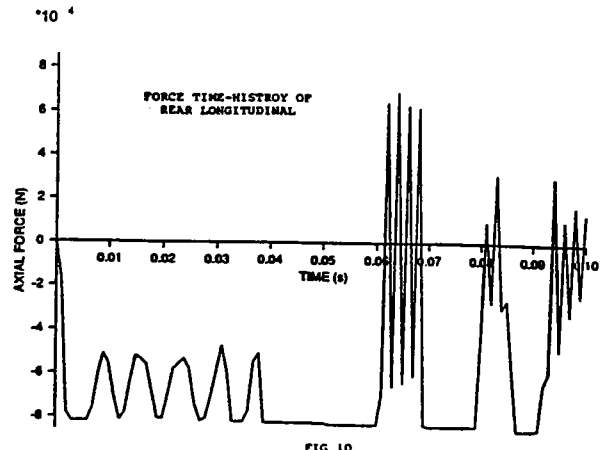


FIG 10

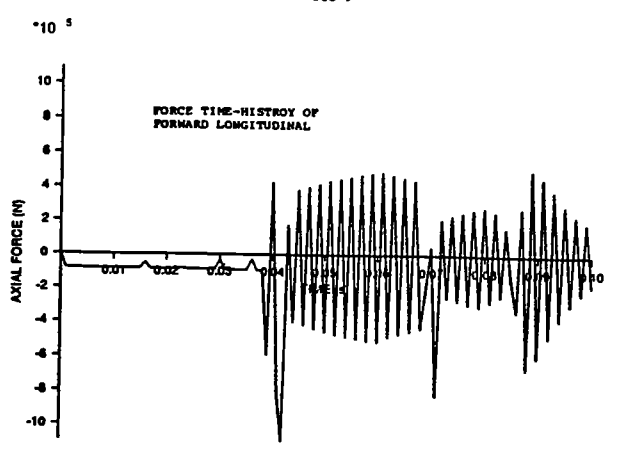


FIG 11

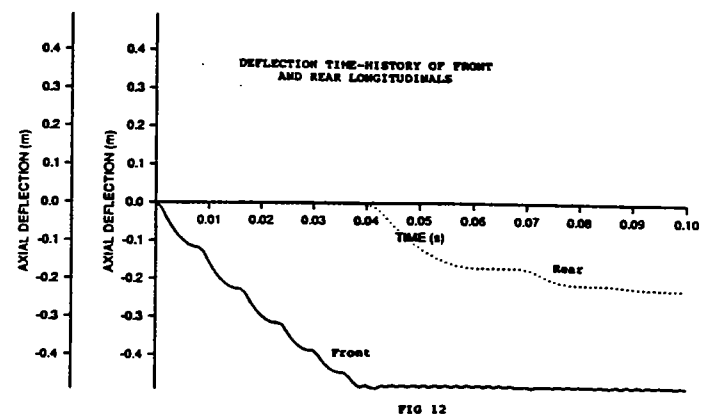


FIG 12

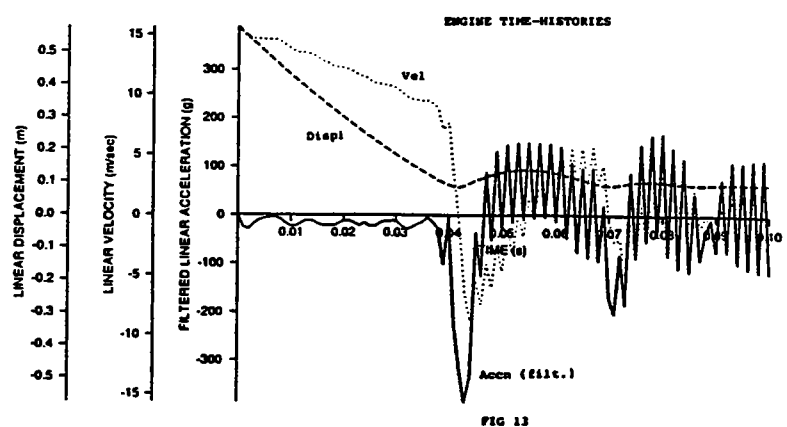


FIG 13

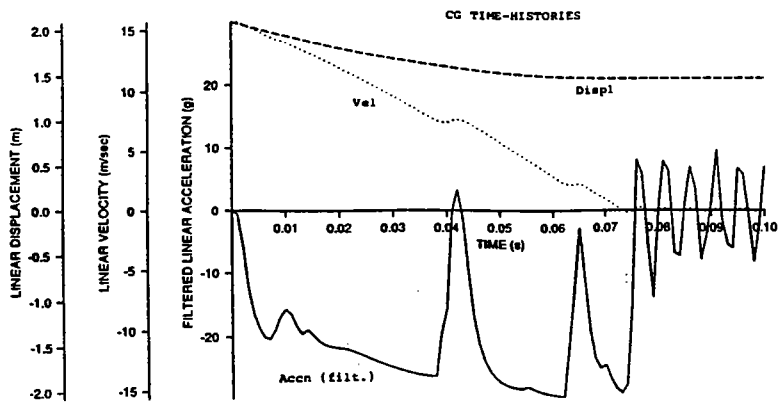


FIG 14

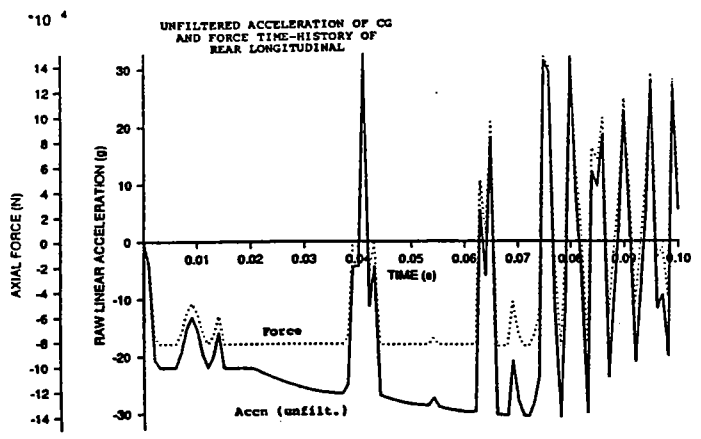


FIG 15

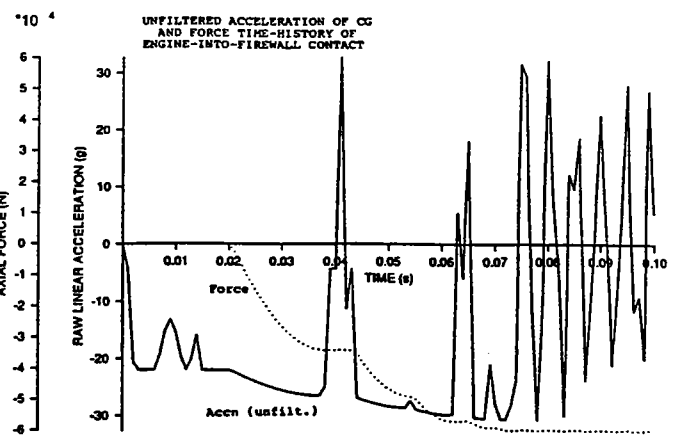


FIG 16

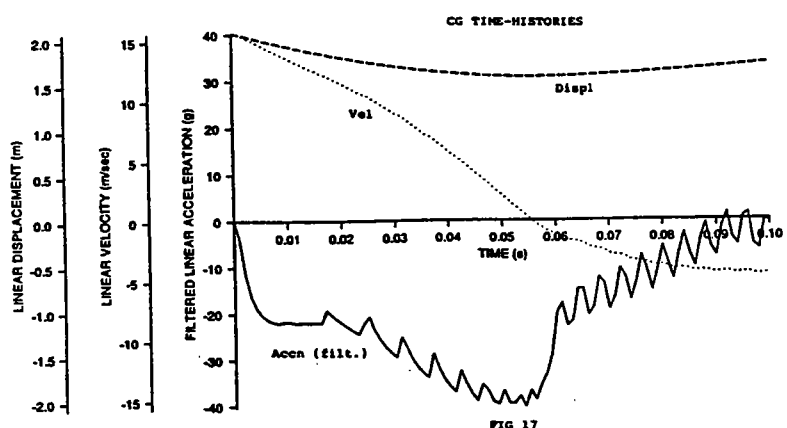


FIG 17

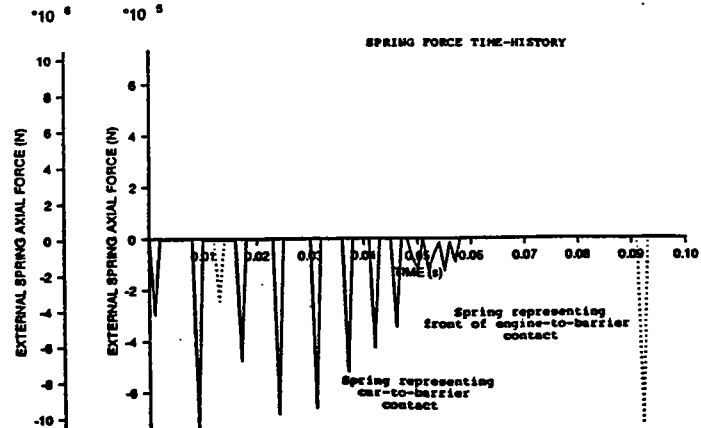


FIG 18

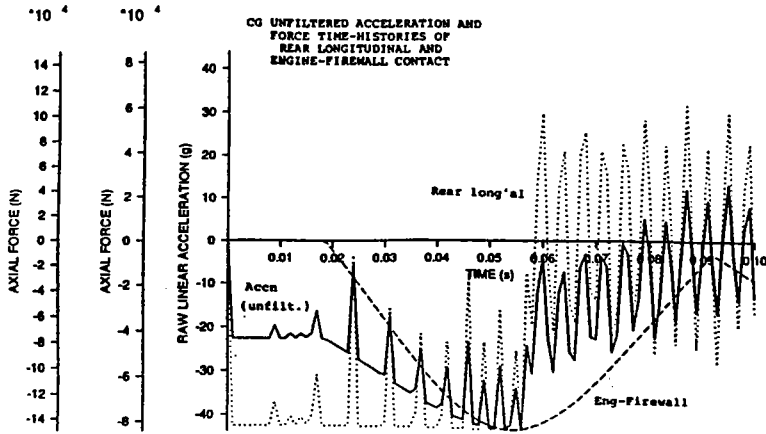


FIG 19

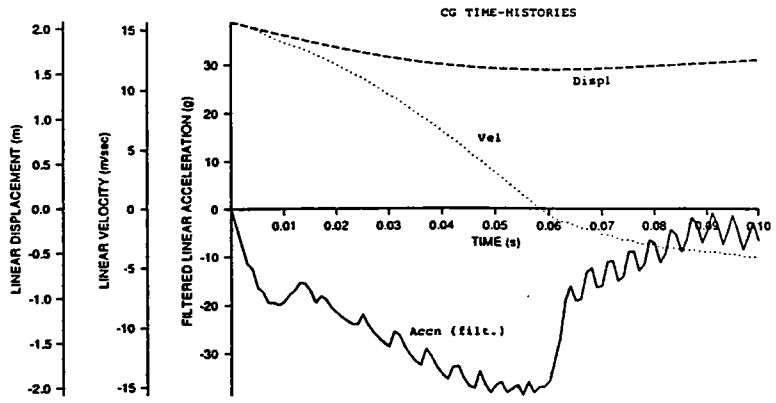


FIG 20

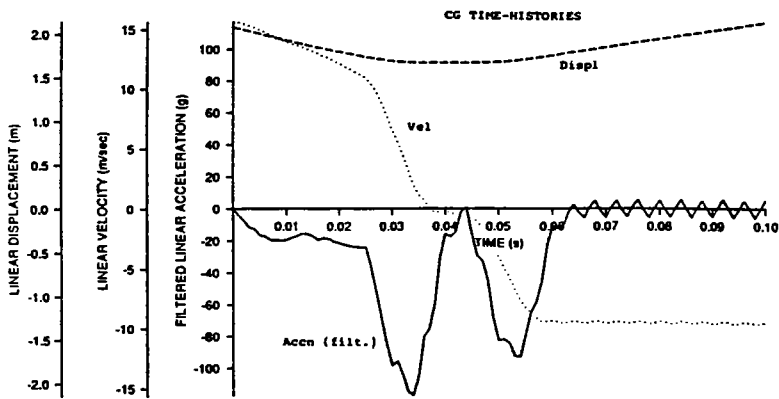


FIG 21

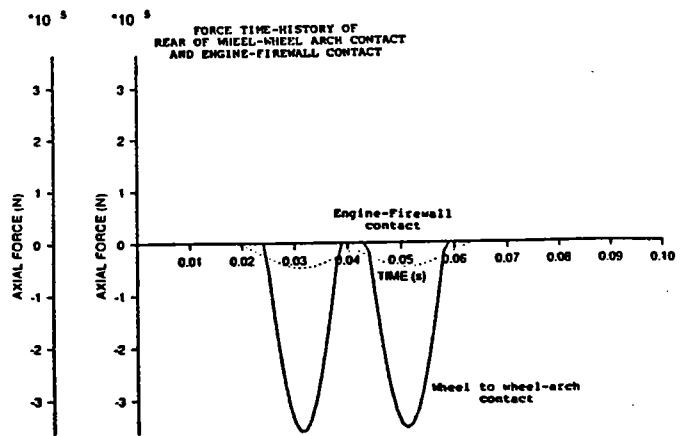


FIG 22

CG TIME-HISTORIES

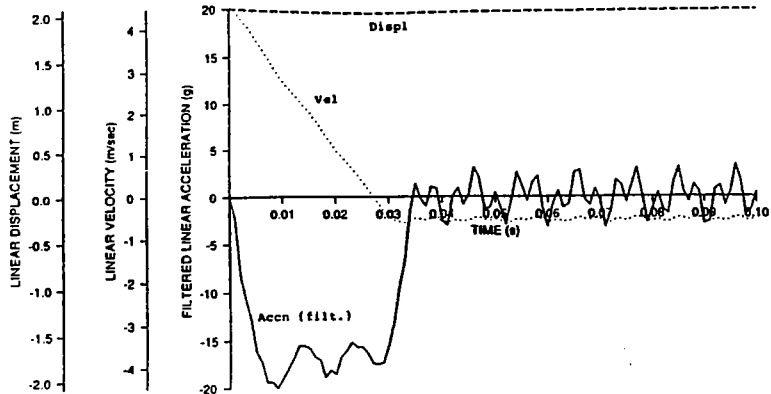


FIG 23